Phosphorylation of SNAP-23 at Ser95 causes a structural alteration and negatively regulates Fc receptor–mediated phagosome formation and maturation in macrophages

Chiye Sakurai[a,b], Makoto Itakura[c], Daiki Kinoshita[a], Seisuke Arai[b], Hitoshi Hashimoto[b], Ikuo Wada[b], and Kiyotaka Hatsuzawa[a,b,*]

[a]Division of Molecular Biology, School of Life Sciences, Faculty of Medicine, Tottori University, Yonago, Tottori 683-8503, Japan; [b]Department of Cell Science, Institute of Biomedical Science, Fukushima Medical University School of Medicine, Fukushima 960-1295, Japan; [c]Department of Biochemistry, Kitasato University School of Medicine, Sagamihara, Kanagawa 228-8555, Japan

ABSTRACT **SNAP-23 is a plasma membrane-localized soluble *N*-ethylmaleimide–sensitive factor attachment protein receptors (SNARE) involved in Fc receptor (FcR)-mediated phagocytosis. However, the regulatory mechanism underlying its function remains elusive. Using phosphorylation-specific antibodies, SNAP-23 was found to be phosphorylated at Ser95 in macrophages. To understand the role of this phosphorylation, we established macrophage lines overexpressing the nonphosphorylatable S95A or the phosphomimicking S95D mutation. The efficiency of phagosome formation and maturation was severely reduced in SNAP-23-S95D–overexpressing cells. To examine whether phosphorylation at Ser95 affected SNAP-23 structure, we constructed intramolecular Förster resonance energy transfer (FRET) probes of SNAP-23 designed to evaluate the approximation of the N termini of the two SNARE motifs. Interestingly, a high FRET efficiency was detected on the membrane when the S95D probe was used, indicating that phosphorylation at Ser95 caused a dynamic structural shift to the closed form. Coexpression of IκB kinase (IKK) 2 enhanced the FRET efficiency of the wild-type probe on the phagosome membrane. Furthermore, the enhanced phagosomal FRET signal in interferon-γ–activated macrophages was largely dependent on IKK2, and this kinase mediated a delay in phagosome-lysosome fusion. These results suggested that SNAP-23 phosphorylation at Ser95 played an important role in the regulation of SNARE-dependent membrane fusion during FcR-mediated phagocytosis.**

Monitoring Editor
Jean E. Gruenberg
University of Geneva

Received: Aug 21, 2017
Revised: May 3, 2018
Accepted: May 8, 2018

This article was published online ahead of print in MBoC in Press (http://www.molbiolcell.org/cgi/doi/10.1091/mbc.E17-08-0523) on May 17, 2018.

The authors declare no conflict of interest.

*Address correspondence to: Kiyotaka Hatsuzawa (hatsu@tottori-u.ac.jp).

Abbreviations used: FcR, Fc receptor; FRET, Förster resonance energy transfer; IFN-γ, interferon-gamma; IKK2, IκB kinase 2; LPS, lipopolysaccharide; MHC, major histocompatibility complex; NOX, NADPH oxidase; PKC, protein kinase C; PMA, phorbol 12-myristate 13-acetate; RB-dextran, rhodamine B–conjugated dextran; SNAP-23, synaptosomal-associated protein of 23 kDa; SNARE, soluble *N*-ethylmaleimide–sensitive factor attachment protein receptor; VAMP, vesicle-associated membrane protein.

INTRODUCTION

Phagocytosis is the essential function of macrophages whereby large foreign particles, such as various bacteria or other immunoglobulin (Ig)-opsonized targets and cellular debris, are internalized into the cell. To disrupt and digest foreign particles, the nascent phagosomes need to "mature," a process characterized by the generation of microbicidal reactive oxygen species (ROS) and the acquisition of an acidic environment resulting from the fusion of endosomes and lysosomes that contain vacuolar type H^+-ATPase (V-ATPase) and various hydrolases (Jutras and Desjardins, 2005; Haas, 2007; Canton, 2014). Remnant peptides from the particles can serve as antigens to be presented by major histocompatibility complex (MHC) class I and/or class II molecules (Mantegazza *et al.*, 2013). Interestingly, the spectrum of presented antigens is

determined by the activation status of macrophages. For example, phagosomes of interferon-gamma (IFN-γ)-activated mouse macrophages, in which the acquisition of lysosomal hydrolases is delayed, exhibit a higher degree of MHC class I–mediated antigen presentation (cross-presentation) than class II–mediated presentation (Trost *et al.*, 2009). Similar findings have been reported in M1 ("classically activated") macrophages that are activated by IFN-γ and/or lipopolysaccharide (LPS) but not in M2 ("alternatively activated") macrophages (Canton *et al.*, 2014). However, it remains unclear how the fusion of phagosomes with endocytic compartments is regulated in these activated macrophages.

The fusion of intracellular compartment or vesicle membranes with the plasma membrane or newly formed phagosomes, which takes place during phagocytosis, is mediated by several soluble *N*-ethylmaleimide–sensitive factor attachment protein receptors (SNAREs), which are the most common fusogenic proteins that contribute to all forms of membrane traffic (Becker *et al.*, 2005; Hatsuzawa *et al.*, 2006; Stow *et al.*, 2006; Ho *et al.*, 2008; Hatsuzawa *et al.*, 2009; Sakurai *et al.*, 2012). SNAREs form complexes that are required for membrane fusion. These complexes contain coiled-coil bundles consisting of four helices, of which three (Qa-, Qb-, and Qc-SNARE motifs) are from SNAREs of the syntaxin and SNAP-25 families and one (R-SNARE motif) is from the vesicle-associated membrane protein (VAMP, also called synaptobrevin) SNARE family (Fasshauer *et al.*, 1998; Jahn and Scheller, 2006; Hong and Lev, 2014). In macrophages, two plasma membrane-localized SNARE proteins, SNAP-23 (synaptosomal-associated protein of 23 kDa; a Qbc-SNARE) and syntaxin 4 (a Qa-SNARE), have been implicated in phagosome formation (Murray *et al.*, 2005; Sakurai *et al.*, 2012). Specifically, phagosomal SNAP-23 regulates the phagosome maturation process as it, in combination with lysosomal VAMP7 (R-SNARE), mediates phagosome-lysosome fusion (Sakurai *et al.*, 2012). Thus, it is conceivable that delayed maturation, as observed in IFN-γ–activated macrophages, is regulated by SNAP-23; however, little is known about how the function of SNAP-23 itself is regulated.

SNAP-23 is a ubiquitously expressed SNARE that has been classified into the SNAP-25 family. Like SNAP-25, SNAP-23 generally mediates exocytosis of secretory vesicles. Phosphorylation of SNAP-23 is known to occur at Ser23/Thr24 and Ser161 in human thrombin–activated platelets and at Ser95 and Ser120 in rat mast cells (Polgar *et al.*, 2003; Hepp *et al.*, 2005). Suzuki and Verma (2008) showed that IκB kinase (IKK) 2 phosphorylates SNAP-23 at Ser95 and Ser120 to cause degranulation after stimulation of mouse mast cells by FcεRI (also known as high-affinity IgE receptor). Moreover, IKK2 is reportedly responsible for the functions of activated platelets (Liu *et al.*, 2002; Malaver *et al.*, 2009) and for regulating platelet exocytosis through the phosphorylation of SNAP-23 at Ser95 (Karim *et al.*, 2013). In both cell types (mast cells and platelets), SNAP-23 phosphorylation enhances exocytosis by augmenting SNARE complex assembly (Suzuki and Verma, 2008; Karim *et al.*, 2013). In contrast, Ca^{2+}-dependent exocytosis in rat astrocytes is inhibited by phorbol 12-myristate 13-acetate (PMA), an activator of protein kinase C (PKC), which is the enzyme responsible for SNAP-23 phosphorylation (Yasuda *et al.*, 2011). In macrophages, however, the role of SNAP-23 phosphorylation during phagocytosis is poorly understood.

In the present study, we demonstrated that the conserved Ser95 of SNAP-23 was phosphorylated in macrophages and that ectopic expression of a phosphomimicking mutant negatively regulated phagosome formation and maturation. On IFN-γ activation, phagosomal SNAP-23 was largely phosphorylated by IKK2, and this caused a significant delay in phagosome–lysosome fusion. These data suggested that SNAP-23 phosphorylation may be crucial for appropriate phagosome formation and maturation during Fc receptor (FcR)-mediated phagocytosis in macrophages.

RESULTS

SNAP-23 was phosphorylated at Ser95 in macrophages

The fusion-promoting activity of SNAP-23 is reportedly regulated by phosphorylation in several cell types. In mast cells, SNAP-23 phosphorylation enhances membrane fusion by facilitating the formation of a SNARE complex (Suzuki and Verma, 2008); this was previously shown (Puri and Roche, 2006) to be required for mast cell exocytosis, whereas an increase in SNAP-23 phosphorylation due to treatment with PMA negatively regulates Ca^{2+}-induced exocytosis in astrocytes (Yasuda *et al.*, 2011). As Ser95 of SNAP-23 is a conserved phosphorylation site between humans and rodents (rats, mice, and hamsters), we first confirmed the phosphorylation at this site in macrophages. Using an anti-phospho-Ser95-SNAP-23 antibody (Yasuda *et al.*, 2011), we detected phosphorylation of SNAP-23 at Ser95 in mouse macrophage-like J774 cells stimulated with PMA (Figure 1A). Next, to determine whether phosphorylation of SNAP-23 at Ser95 regulated phagosome formation and maturation in macrophages, we established transfectants stably expressing monomeric Venus (mVenus)-tagged SNAP-23 (mV-S23) proteins consisting of either the wild-type (WT) sequence, the nonphosphorylatable S95A (serine replaced by alanine) mutation, or the phosphomimicking S95D (serine replaced by aspartate) mutation at similar levels (Figure 1B, top). As expected, the anti-phospho-Ser95-SNAP-23 antibody did not detect phosphorylation in cells expressing either of the phosphomutants, even on PMA stimulation (Figure 1B, bottom). As shown in Figure 1C, the mV-S23 proteins were mostly observed on

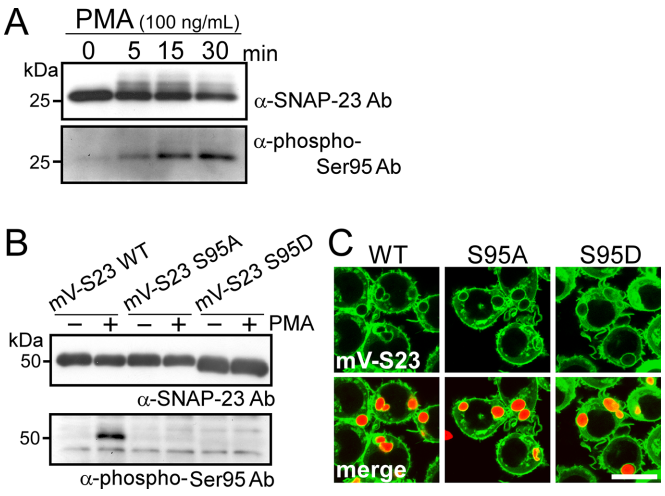

FIGURE 1: SNAP-23 was phosphorylated at Ser95 in macrophages. (A) J774 cells were incubated for the indicated times in the presence of PMA. Total lysates were analyzed by Western blotting using antibodies against SNAP-23 and phospho-Ser95-SNAP-23. (B) Establishment of J774 cells expressing mVenus-tagged proteins (mV-S23-WT, mV-S23-S95A, or mV-S23-S95D). Transfectants were incubated for 30 min in the presence or absence of PMA at a final concentration of 100 ng/ml. Phosphorylation of the mV-S23 proteins was analyzed by Western blotting using the indicated antibodies. (C) Live-cell imaging during phagocytosis of IgG-opsonized Texas Red–zymosan particles by J774 cells did not reveal differences in the intracellular localization of the three mV-S23 proteins. Bar, 10 μm.

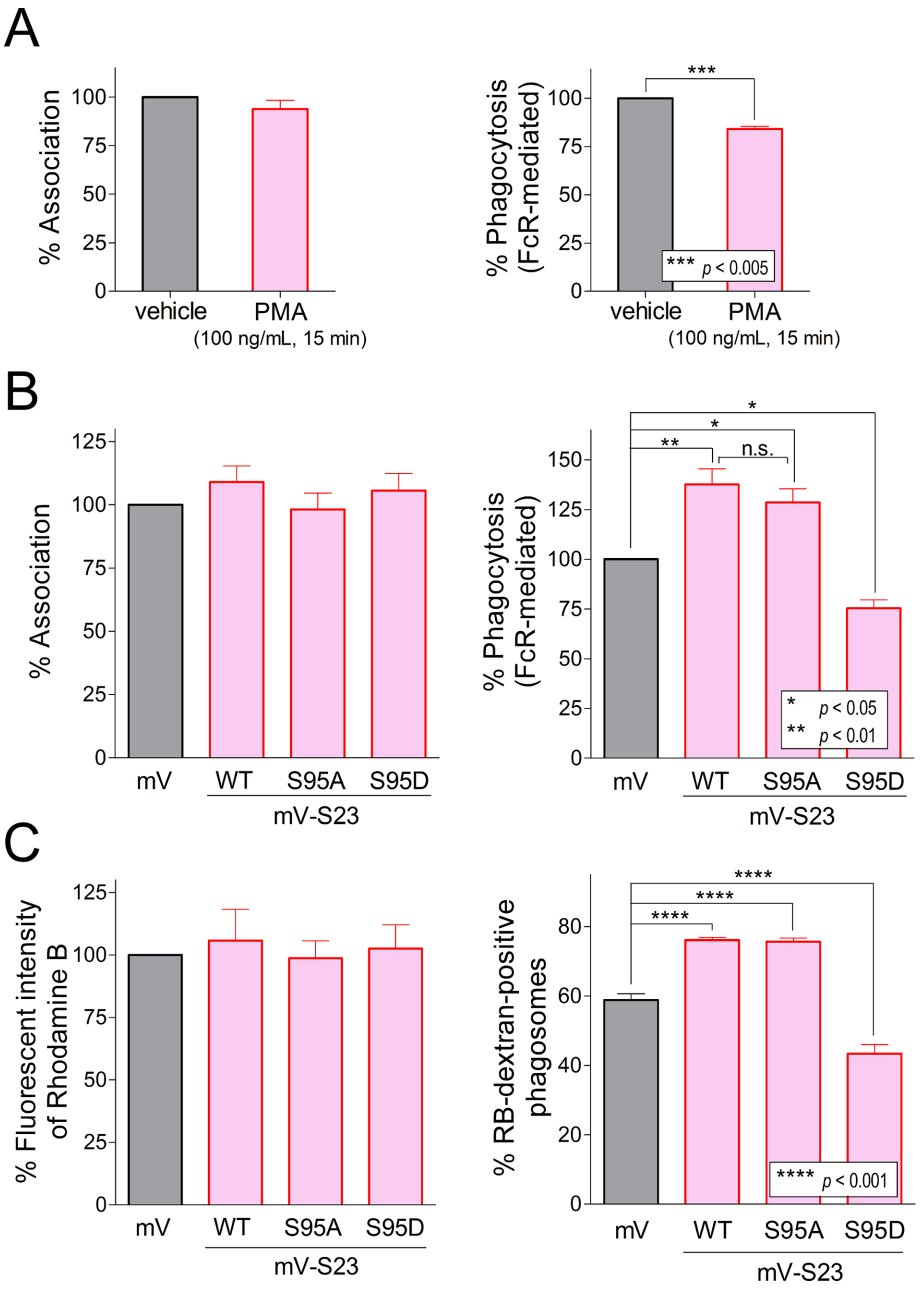

FIGURE 2: Overexpression of the phosphomimicking SNAP-23-S95D mutant reduced FcR-mediated phagocytosis and delayed phagosome maturation. (A) J774 cells were incubated for 15 min in the presence or absence of PMA (100 ng/ml) at 37°C, followed by replacement with fresh medium containing IgG-opsonized Texas Red–zymosan–labeled particles. After incubation with the particles, the efficiencies (%) of association (left) and FcR-mediated phagocytosis (right) were measured as described under *Materials and Methods*. Fluorescence values were normalized to the maximum value obtained from cells treated with vehicle, which was arbitrarily defined as 100%. Data presented are the mean ± SE of four to five independent experiments. (B) J774 cells expressing mV-tagged proteins were incubated with IgG-opsonized Texas Red–zymosan particles, and the efficiencies (%) of association (left) and phagocytosis (right) were measured. Data presented are the means ± SEs from five to six independent experiments. (C) J774 cells expressing mV-tagged proteins were incubated with RB-dextran for 8 h, followed by chase in fresh growth medium without dextran for 5 h to label late endosomes/lysosomes. Total RB fluorescence was measured (left) to serve as an indicator of labeling efficiency. Data presented are the means ± SEs of four independent experiments. The percentage of RB–dextran–positive phagosomes (more than 30 individual phagosomes from at least 30 different cells were measured in each experiment) was calculated (right). Data presented are the means ± SEs of seven independent experiments. Statistical analyses were carried out using two-tailed, paired Student's *t* tests (for experiments with two groups, panel A, right) or one-way ANOVA with Tukey's post-hoc test (for experiments with more than two groups, panels B, right, and C, right).

the plasma membrane and on phagosomes containing IgG-opsonized Texas Red–conjugated zymosan particles, and the localization of both mutants was indistinguishable from that of the WT protein (Supplemental Figure S1A).

SNAP-23 phosphorylation has been reported to enhance the formation of complexes between SNAP-23 and cognate SNARE proteins (Hepp *et al.*, 2005; Suzuki and Verma, 2008; Karim *et al.*, 2013; Wesolowski and Paumet, 2014). Thus, to investigate the effect of SNAP-23 phosphorylation on its interaction with other SNARE proteins in resting macrophages, we performed coimmunoprecipitation experiments using total lysates from the mV-S23 transfectants (expressing either SNAP-23 WT or phosphomutants), in which we assessed the interaction between each of these mV-S23 proteins with plasma membrane- and endocytic membrane-localized SNAREs that have been previously shown to interact with SNAP-23 (Sakurai *et al.*, 2012). Interestingly, both the phosphomimicking mV-S23-S95D mutant and the nonphosphorylatable S95A mutant interacted with plasma membrane-localized SNAREs (syntaxin 3, syntaxin 4, syntaxin 11, and VAMP5) and endocytic membrane-localized SNAREs (syntaxin 7, syntaxin 13, VAMP3, VAMP4, VAMP7, and VAMP8), similarly to that observed with mV-S23 WT (Supplemental Figure S2). This suggested that the phosphorylation status at Ser95 did not affect the localization of SNAP-23 and its interaction with other SNARE proteins in macrophages, contrary to what has been observed in other types of cells.

Phosphorylation of SNAP-23 at Ser95 inhibited phagosome formation and maturation during FcR-mediated phagocytosis

To investigate the effects of activated PKC on FcR-mediated phagocytosis in J774 cells, the opsonized Texas Red–conjugated zymosan assay was performed in cells stimulated with PMA (100 ng/ml, 15 min) to ensure that SNAP-23 was phosphorylated at Ser95 (Figure 1A). PMA reduced the efficiency of phagocytosis by 15.92% ± 1.45% (Figure 2A, right) without affecting the association index of zymosan particles with the cell surface (Figure 2A, left). This suggested that SNAP-23 phosphorylation may negatively regulate phagosome formation. To confirm this, we assessed phagocytosis efficiency in the phospho-mutant-expressing transfectants. Both mV-S23-S95A– and mV-S23-S95D–expressing cells displayed association efficiencies similarly to that of

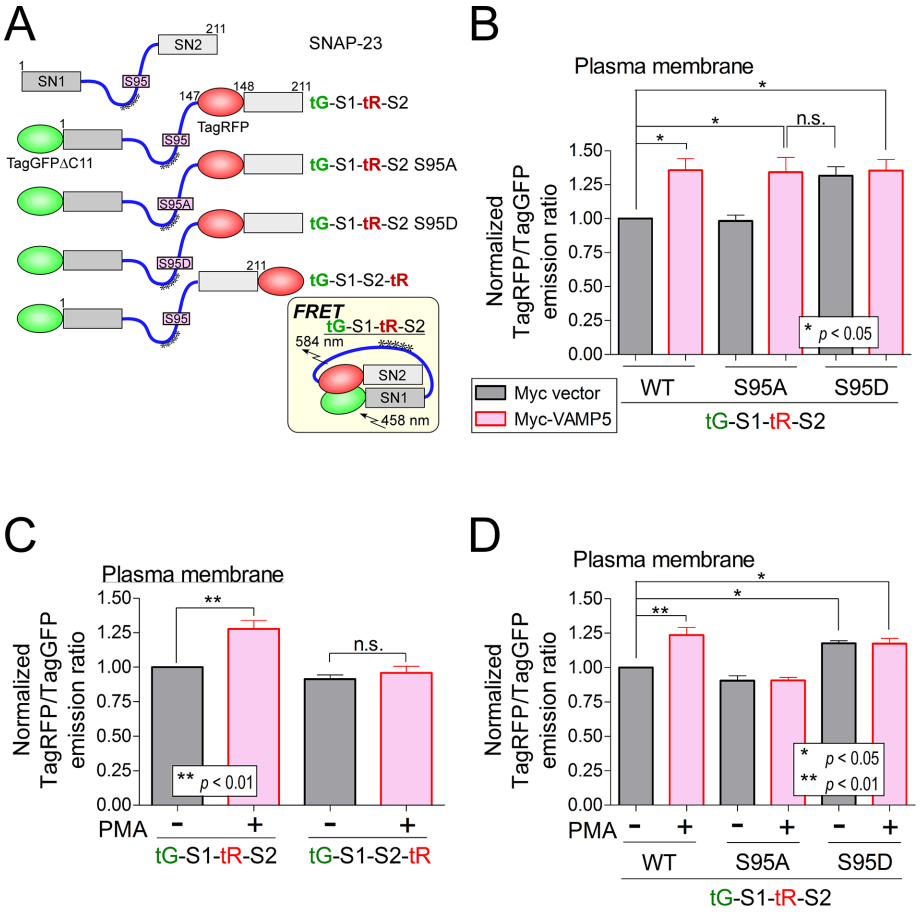

FIGURE 3: The FRET signal of SNAP-23 probe on the plasma membrane was dependent on its phosphorylation status at Ser95 in PMA-stimulated J774 cells. (A) Schematic of the SNAP-23 FRET probes used in this study. As described previously, truncated TagGFP2 (TagGFPΔC11) and TagRFP were fused to SNAP-23 (Sakurai *et al.*, 2012). The inset shows the predicted conformation of the SNAP-23-based FRET construct (tG-S1-tR-S2) on formation of the fusogenic SNARE complex. Asterisks indicate potentially palmitoylated cysteine residues. (B–D) J774 cells were transiently transfected with SNAP-23 FRET probes alone (C, D) or in combination with Myc constructs (B). The spectroscopic function of a laser-scanning microscope was used to excite the plasma membranes of living cells at 458 nm and the resulting emission spectra were analyzed. In C and D, measurements of the spectra from the plasma membranes were performed after treatment with PMA (100 ng/ml) for 15 min. The emission peak of TagRFP (at 580 or 581 nm) was divided by that of TagGFP2 (at 505 or 502 nm) (TagRFP/TagGFP) and normalized to the value obtained from cells expressing the tG-S1-tR-S2 WT with the Myc vector (B) or in the absence of PMA (C, D) in the same respective experiment, which was arbitrarily set to 1.00. Data presented are the means ± SEs of three to five independent experiments. Statistical analyses were carried out using one-way ANOVA with Tukey's post-hoc test (for experiments with more than two groups, panels B, C, and D).

mV-S23 WT-expressing cells (Figure 2B, left). Consistent with this result, immunofluorescence microscopy revealed a similar expression and localization of CD64 (Fcγ receptor Ia) on the plasma membrane in these cells (Supplemental Figure S1B). With respect to phagocytosis efficiency, mV-S23-S95A-expressing cells showed almost identical values to mV-S23-WT-expressing cells, which was significantly higher than that in control cells expressing mVenus (mV; Figure 2B, right) (Sakurai *et al.*, 2012). In contrast, mV-S23-S95D-expressing cells displayed significantly lower phagocytosis efficiencies than control cells (Figure 2B, right). Similar effects of overexpressing mV-S23-WT and mV-S23-S95D on phagocytosis efficiency were observed even at early time points (within 30 min) during FcR-mediated phagocytosis (Supplemental Figure S3). These results suggested that the phosphorylation of SNAP-23 at Ser95 negatively regulated fusion of the plasma membrane with intracellular vesicles or organelles to form phagosomes during FcR-mediated phagocytosis.

Since SNAP-23 has been shown to regulate phagosome maturation in macrophages (Sakurai *et al.*, 2012), we also investigated whether the presence of SNAP-23 phosphomutants affected phagosome-lysosome fusion efficiency. For this, we preloaded lysosomes with the fluid-phase marker, rhodamine B (RB)-conjugated to dextran. As shown in Figure 2C, mV-S23-S95D–expressing cells displayed a significant decrease in fusion efficiency compared with that in cells expressing mV-S23-WT or mV-S23-S95A (right panel), without changes in the efficiency of lysosomal labeling with RB-dextran (left panel).

Taken together, these data clearly indicated that phosphorylation of SNAP-23 at Ser95 played an inhibitory role in phagosome formation and maturation during FcR-mediated phagocytosis in macrophages.

Phosphorylation at Ser95 mediated structural alterations in SNAP-23

A possible explanation for the dominant-negative effect of the SNAP-23-S95D mutant on phagosome formation and maturation could be that the presence of the mutant caused acceleration of inappropriate SNARE complex formation or deceleration of indispensable SNARE complex formation. However, coimmunoprecipitation experiments using lysates from J774 cells expressing mV-S23 WT or mutants after ingestion of IgG-opsonized zymosan particles failed to detect any differences in the levels of immunoprecipitated SNARE proteins (Supplemental Figure S4). Next, we investigated whether the overall structure of SNAP-23 was altered by these mutations using a variation of the methods first described by Shcherbo *et al.* (2009). In a previous study (Sakurai *et al.*, 2012), we constructed intramolecular Förster resonance energy transfer (FRET) probes for SNAP-23 in which TagGFP2 (tG) and TagRFP (tR) had been added, as donor and acceptor fluorescence probes, at the N termini of the SN1 and SN2 motifs, respectively (tG-S1-tR-S2; Figure 3A). During the formation of SNARE complexes between SNAP-23 and other partners, which occurs during phagocytosis, the two SNARE motifs (located at 1–75 and 148–211, respectively) come closer, thus increasing the FRET signal from the probe and indicating a structural change (Figure 3A, inset). In our previous study, we showed that even though the FRET signal was observed on both the plasma and phagosomal membranes when the probe was expressed in J774 cells, the signal on the plasma membrane was significantly enhanced when tG-S1-tR-S2 was coexpressed with Myc-VAMP5 (Sakurai *et al.*, 2012). In the current study, to investigate whether structural alterations were

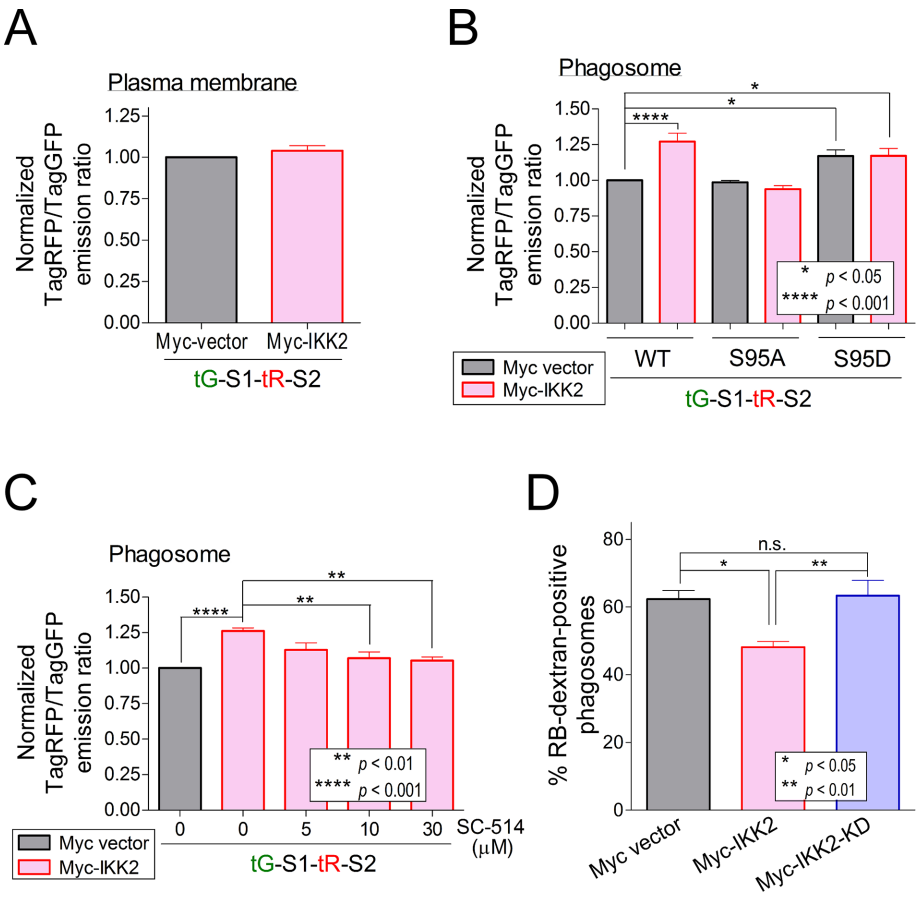

FIGURE 4: Structural alteration of phagosomal SNAP-23 caused by IKK2 reduced the efficiency of phagosome maturation. (A) J774 cells were transiently cotransfected with a SNAP-23 tG-S1-tR-S2 probe and Myc-IKK2, which was followed by determination of the FRET efficiency on the plasma membrane of living cells. (B, C) J774 cells cotransfected with SNAP-23 probes and Myc-IKK2 were incubated with IgG-opsonized zymosan particles at 37°C for 20 min, in the presence (C) or absence (B) of SC-514 at the indicated concentrations, and the FRET efficiency on the phagosome membrane of living cells was then measured. Data presented are the means ± SEs of four to five independent experiments. (D) J774 cells labeled with RB–dextran were transiently transfected with an empty Myc vector, Myc-IKK2, or Myc-IKK2-KD (kinase dead) and then subjected to phagosome-lysosome fusion assays as described in Figure 2C. Data presented are the means ± SEs of six independent experiments. Statistical analyses were carried out using one-way ANOVA with Tukey's post-hoc test (for experiments with more than two groups, panels B, C, and D).

caused by phosphorylation of SNAP-23 at Ser95, SNAP-23 phosphomutant probes were also constructed (Figure 3A; tG-S1-tR-S2 S95A and tG-S1-tR-S2 S95D). As shown in Figure 3B, coexpression with Myc-VAMP5 enhanced the FRET signal from the S95A probe on the plasma membrane, similar to that observed for the WT probe (Sakurai *et al.*, 2012), suggesting that these VAMP5-dependent increases in FRET signal were most likely independent of phosphorylation at Ser95. In contrast, when J774 cells expressing the WT or mutant probe were stimulated with PMA, which caused phosphorylation of SNAP-23 at Ser95 (Figure 1A), significantly enhanced FRET efficiency on the plasma membrane was observed in cells expressing the WT probe (Figure 3C and Supplemental Figure S5, A and B) compared with that with the negative control probe (tG-S1-S2-tR), whereas the S95A probe showed no increase (Figure 3D). These results implied that the PMA-induced increase in FRET signal intensity was completely dependent on phosphorylation at Ser95. Unexpectedly, the S95D probe showed a constitutively high FRET signal intensity, independent of coexpression with Myc-VAMP5 (Figure 3B) or PMA-stimulation (Figure 3D). This constitutive high FRET was confirmed by ratiometric imaging analysis (Supplemental Figure S5C). To investigate whether the enhanced signal resulted from misfolding of SNAP-23 caused by the S95D mutation, we constructed two other probes, tG-S1-tR-S2 ΔCys and tG-S1-tR-S2 ΔCys S95D, based on the SNAP-23 ΔCys mutant in which five cysteine residues, candidates for palmitoylation, were replaced with serine residues (Supplemental Figure S6A). The ΔCys mutation does not allow SNAP-23 to bind to membranes (either plasma or phagosomal); thus, both SNAP-23 ΔCys-based probes remained in the cytoplasm (data not shown). With this cytoplasmic form, the WT and S95D probes did not display any differences in FRET signal intensity (Supplemental Figure S6B). Thus, the enhanced FRET signal from the tG-S1-tR-S2 S95D probe could not be attributed to misfolding caused by the S95D mutation but rather may result from an interaction with some factor on the membrane.

These results suggested that phosphorylation of SNAP-23 at Ser95 caused a structural shift to a closed conformation in macrophages.

IKK2 phosphorylated phagosomal SNAP-23 at Ser95 to reduce phagosome-lysosome fusion efficiency

Past studies have shown that the kinase activity of PKC is required for the phosphorylation of SNAP-23 at Ser95 during the regulation of exocytosis in astroglial cells (Yasuda *et al.*, 2011), whereas phosphorylation by IKK2 enhances secretion in mast cells and platelets (Suzuki and Verma, 2008; Karim *et al.*, 2013). More recently, it was reported that Toll-like receptor (TLR) signaling activates IKK2 in dendritic cells, which then mediates the phosphorylation of phagosomal-localized SNAP-23 (Nair-Gupta *et al.*, 2014). In the current study, to assess whether IKK2 was responsible for the phosphorylation of SNAP-23 at Ser95 in macrophages, we performed FRET analysis in J774 cells transiently coexpressing a tG-S1-tR-S2 probe (WT, S95S, or S95D) and Myc-IKK2. When coexpressed with the WT probe, Myc-IKK2 did not enhance the FRET signal on the plasma membrane, as the observed signal was similar to that detected when the probe was coexpressed with an empty Myc vector (Figure 4A). In contrast, a significantly enhanced FRET signal was detected on phagosomes containing IgG-opsonized zymosan. This increase in the FRET signal from the phagosome membranes was not observed with the S95A probe (Figure 4B), indicating that Ser95 may be important for the structural alteration of phagosomal membrane-localized SNAP-23 caused by coexpression with Myc-IKK2. In the case of the S95D probe, an enhanced FRET signal from the phagosomal membrane was observed independently of whether the probe was coexpressed with Myc-IKK2 or empty Myc vector (Figure 4B).

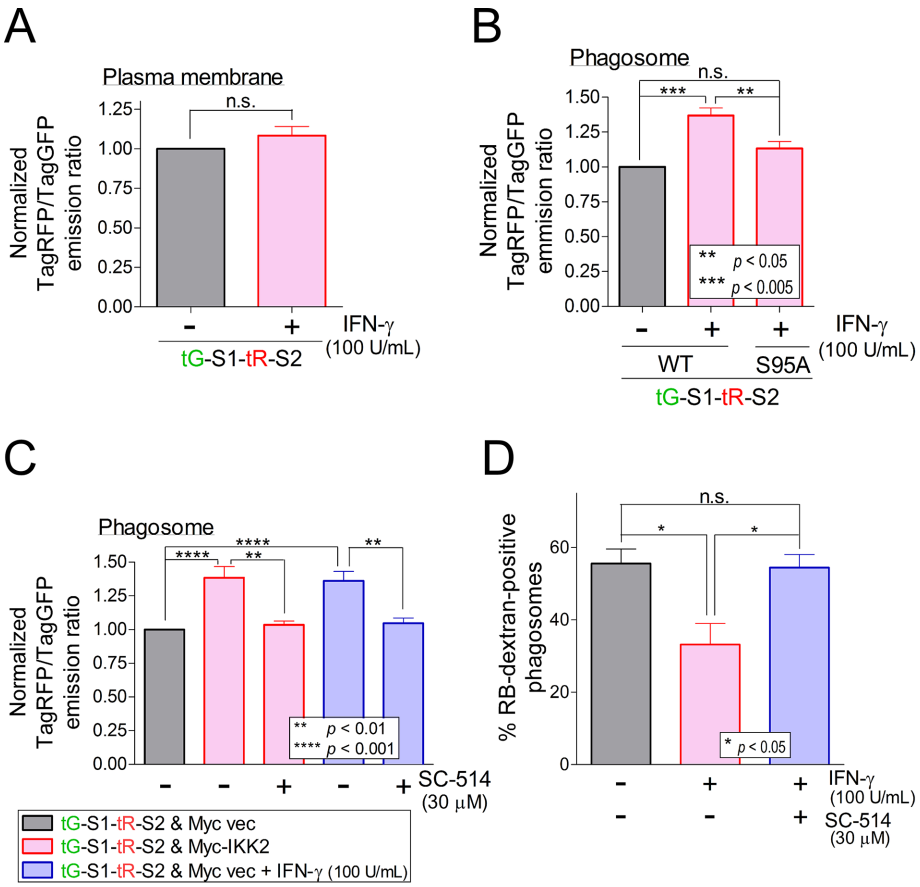

FIGURE 5: Structural alteration of phagosomal SNAP-23 in IFN-γ–activated macrophages was partially dependent on IKK2 activity and caused a delay in phagosome maturation. (A, B) J774 cells were transiently transfected with SNAP-23 probes and incubated in the presence or absence of IFN-γ (100 U/ml). Eighteen hours after transfection, the FRET efficiency of living cells on the plasma membrane (A) or on the membrane of phagosomes containing IgG-opsonized zymosan particles (B) was analyzed as described under *Materials and Methods*. Data presented are the means ± SEs of 7 to 10 independent experiments. (C) J774 cells coexpressing the SNAP-23 tG-S1-tR-S2 probe and a Myc-tagged construct (empty vector or Myc-IKK2) were incubated in the presence or absence of IFN-γ (100 U/ml). Eighteen hours after transfection, the cells were incubated with IgG-opsonized zymosan particles in the presence or absence of SC-514 (30 μM) at 37°C for 20 min, and, subsequently, the FRET efficiency on the phagosome membranes of living cells was analyzed. Data presented are the means ± SEs of three independent experiments. (D) J774 cells labeled with RB–dextran were incubated in the presence or absence of IFN-γ (100 U/ml) for 18 h and then subjected to phagosome-lysosome fusion assays as described in Figure 2C. IFN-γ–activated cells were preincubated in the presence or absence of SC-514 (30 μM) at 37°C for 20 min before and during the assay. Data presented are the means ± SEs of four independent experiments. Statistical analyses were carried out using two-tailed, paired Student's *t* tests (for experiments with two groups, panel A) or one-way ANOVA with Tukey's post-hoc test (for experiments with more than two groups, panels B, C, and D).

Next, to examine whether the enhanced phagosomal FRET signal from the WT probe was caused by the enzymatic activity of IKK2, FRET measurements were repeated in the presence of SC-514, a selective IKK2 inhibitor. The inhibitor markedly blocked the Myc-IKK2–induced enhancement of the FRET signal from the WT probe in a concentration-dependent manner (Figure 4C). This suggested that the kinase activity of IKK2 was indeed responsible for the phosphorylation of phagosomal SNAP-23 at Ser95 in macrophages. Given the inhibitory effects of the SNAP-23-S95D mutant on phagosome maturation (Figure 2C), IKK2 may also delay phagosome maturation by reducing phagosome-lysosome fusion efficiency. To test this hypothesis, IKK2 or a kinase-dead mutant (IKK2-KD), in which Lys44 was replaced by methionine (Mercurio *et al.*, 1997), was expressed in macrophages. Using a microscope, phagosomes (both RB-dextran-positive and unlabeled) containing IgG-opsonized beads were counted in J774 cells expressing mVenus as a marker and cotransfected with Myc-vectors (empty, IKK2, or IKK2-KD). As shown in Figure 4D, Myc-IKK2 significantly decreased the number of RB-dextran-positive phagosomes compared with that with the empty Myc-vector, whereas Myc-IKK2 KD had no effect, indicating that the kinase activity of IKK2 was involved in the delay in phagosome-lysosome fusion. Taken together, these results suggested that IKK2 phosphorylated phagosomal SNAP-23 at Ser95 to reduce the phagosome-lysosome fusion efficiency. However, neither the phagosomal localization of ectopically expressed IKK2 (data not shown) nor the interaction between mV-S23 proteins and endogenous IKK2 (Supplemental Figure S4) was detected in our system.

IFN-γ induced a structural alteration in SNAP-23 and a delay in phagosome maturation

IFN-γ is a T-helper 1 cytokine that regulates the antimicrobial activity of macrophages by modulating functions such as pathogen uptake and antigen presentation. Macrophages activated with IFN-γ exhibit neutralization of phagosomal pH and a delay in the fusion of phagosomes with lysosomes during phagocytosis (Trost *et al.*, 2009; Canton *et al.*, 2014). Even though phagosomal SNAP-23 has been shown to be phosphorylated in IFN-γ–activated macrophages (Trost *et al.*, 2009), the physiological significance of this event remains unknown. These reports prompted us to perform FRET analysis on macrophages expressing the SNAP-23 tG-S1-tR-S2 probes in the presence of IFN-γ. When J774 cells were transfected with the WT probe and then activated with IFN-γ (+IFN-γ) for 18 h, FRET efficiency on their plasma membranes was slightly higher compared with that of resting cells (–IFN-γ); however, the difference was not statistically significant (Figure 5A). In contrast, the FRET signal on phagosomes was clearly enhanced. In IFN-γ–activated cells transfected with the S95A probe, the phagosomal FRET signal was markedly lower than that in IFN-γ–activated cells expressing the WT probe (Figure 5B). This result suggested that the observed FRET signal from the SNAP-23 WT probe was largely dependent on the phosphorylation of SNAP-23 at Ser95. As shown in Figure 5C, both the IFN-γ- and Myc-IKK2–induced increases in FRET signal from the WT probe were significantly reduced in the presence of SC-514 (blue and red columns, respectively),

indicating that endogenous IKK2 kinase activity was indispensable for the IFN-γ–dependent phosphorylation of phagosomal SNAP-23 at Ser95.

Finally, to determine whether IKK2 kinase activity was involved in the maturation of phagosomes in the presence of IFN-γ in macrophages, a phagosome-lysosome fusion assay was performed in IFN-γ–activated J774 cells using IgG-opsonized particles. As shown in Figure 5D, IFN-γ–activated cells displayed markedly lower phagosome-lysosome fusion efficiency compared with resting cells, whereas this reduction was significantly reversed when IKK2 activity was impaired by SC-514 treatment. Consistent with this, the reduced efficiency of phagosomal acidification (LysoTracker-positive phagosomes) in IFN-γ–activated cells was also reversed by SC-514 treatment (Supplemental Figure S7). These results suggested that phosphorylation of phagosomal SNAP-23 by IKK2 was required for the IFN-γ–induced delay in phagosome maturation during FcR-mediated phagocytosis in macrophages.

DISCUSSION

In this study, we found that the phosphorylation of plasma membrane-localized SNAP-23 at Ser95 impeded phagocytosis in macrophages (Figure 2). Previous studies reported a positive role for SNAP-23 phosphorylation in several types of regulated exocytosis in cells such as platelets (Polgar *et al.*, 2003; Hepp *et al.*, 2005; Karim *et al.*, 2013) and mast cells (Hepp *et al.*, 2005; Suzuki and Verma, 2008), whereas this phosphorylation mediates PKC-dependent inhibition of Ca^{2+}-dependent exocytosis in astrocytes (Yasuda *et al.*, 2011). In regulated exocytosis, PKC or IKK2 is responsible for SNAP-23 phosphorylation. The results of our FRET analyses in macrophages indicated that the ectopic expression of IKK2 did not mediate the phosphorylation of SNAP-23 at Ser95 on the plasma membrane (Figure 4A). Presumably, kinases other than IKK2, such as PKC, may regulate SNAP-23 phosphorylation on the plasma membrane to reduce the efficiency of FcR-mediated phagocytosis (Figure 2A). Previously, we showed that overexpression of SNAP-23 in PMA-activated J774 cells enhances the release of ROS from the cells to the extracellular space (Sakurai *et al.*, 2012), suggesting that SNAP-23 phosphorylated by PKC may preferentially regulate exocytic membrane fusion to form a NADPH oxidase 2 (NOX2) complex on the plasma membrane, thus becoming unavailable for phagosome formation (Figure 2A). Recently, researchers showed that the suppression of FcR-mediated phagocytosis in J774 cells treated with PMA is caused by inactivation of the small GTPase Rac, an inducer of actin polymerization. The activation of Rac is suppressed by PKC-dependent activation of SHP1 phosphatase (Joshi *et al.*, 2014). These findings indicate that both membrane fusion and actin polymerization via PKC signaling appear to regulate FcR-mediated phagocytosis in J774 cells, although the role of PKC in phagocytosis is still under debate (Larsen *et al.*, 2000, 2002; Wood *et al.*, 2013). Alternatively, phagocytic receptors other than FcR may activate some PKCs when they bind to their targets at the plasma membrane to facilitate SNAP-23 phosphorylation. In either case, once phosphorylated at Ser95, SNAP-23 may no longer be involved in FcR-mediated phagocytosis (Figure 6). If both targets of FcR and targets of other receptors, such as Toll-like receptors, coexist, then it may be possible to engulf the latter target preferentially over IgG-opsonized targets via phosphorylated SNAP-23 (Figure 6). Indeed, overexpression of SNAP-23-S95D mutant reduced FcR-mediated phagocytosis efficiency. This mutant may compete for assembly of the acceptor complex consisting of endogenous SNAP-23 and SNARE partners, such as syntaxin 4, at the plasma membrane. Moreover, the possibility that the S95D mutant partially suppresses the recycling of FcR from phagosomes cannot be excluded. However, the precise role of SNAP-23 phosphorylation in FcR-mediated phagocytosis remains unclear.

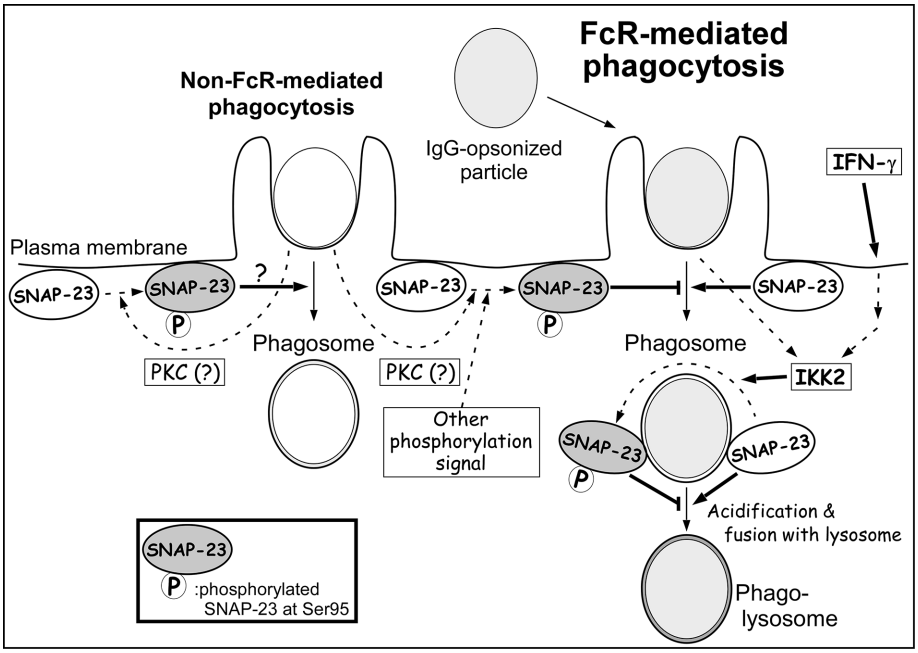

FIGURE 6: Schematic representation of SNAP-23–mediated regulation of phagosome formation and maturation during FcR-mediated phagocytosis in macrophages. Formation of a phagosome containing an IgG-opsonized particle is induced by SNAP-23 without phosphorylation at Ser95. Phosphorylation of SNAP-23 by other factors, such as PKC, suppresses its ability to regulate phagosome formation. In the presence of both IgG-opsonized and nonopsonized particles, a non-FcR–mediated phagocytosis pathway may allow phosphorylated SNAP-23 to induce phagosome formation, resulting in the suppression of FcR-mediated phagocytosis. Although SNAP-23 in resting macrophages facilitates phagosome maturation, this process is suppressed or delayed by the phosphorylation of SNAP-23 at Ser95 by IKK2 in IFN-γ–activated macrophages (see *Discussion*).

We demonstrated reduced phagosome-lysosome fusion efficiency for the SNAP-23-S95D mutant, indicating that phagosome maturation was delayed by SNAP-23 phosphorylation at Ser95. A delay in the maturation of phagosomes has been reported in IFN-γ–activated (Jutras *et al.*, 2008) and IFN-γ/LPS–activated macrophages (Canton *et al.*, 2014), as well as in LPS-activated dendritic cells (Alloatti *et al.*, 2015). Consistent with these studies, we observed reduced efficiency of phagosome-lysosome fusion and phagosomal acidification in J774 macrophages activated with IFN-γ compared with that in resting cells, which was rescued by treatment with SC-514. IFN-γ–activated cells expressing the SNAP-23 WT probe displayed enhanced FRET efficiency on phagosomes compared with

those expressing the SNAP-23-S95A probe; however, FRET signal intensity decreased in the presence of SC-514, suggesting that IKK2 kinase activity was required for the phosphorylation of phagosomal SNAP-23 on IFN-γ activation. Thus, the phosphorylation of SNAP-23 at Ser95 by IKK2 should be at least partly responsible for the suppression of phagosome maturation on IFN-γ signaling (Figure 6). However, a past phagosomal proteome analysis in IFN-γ–activated macrophages revealed the involvement of several types of kinases in the phosphorylation of phagosomal proteins (Trost *et al.*, 2009), suggesting that kinases other than IKK2 may also regulate phagosomal SNAP-23 function. Alternatively, phagosomal PKC isozymes, such as PKC-α and PKC-ε, may regulate IKK2 activity as upstream kinases during phagosome maturation (Ng Yan Hing *et al.*, 2004; Wood *et al.*, 2013).

Phagosomes containing foreign particles gradually mature by acquiring a set of phagosomal proteins that generate ROS, lower the phagosomal pH, and digest foreign proteins. These include the NOX2 complex, the vacuolar type H^+-ATPase, some MHC molecules, and lysosomal hydrolases/proteases. The progression of phagosomal maturation depends on the activation status of the macrophages. Phagosomes of IFN-γ–activated murine macrophages display delayed acquisition of lysosomal markers, such as LAMP-1 and β-hexosaminidase A, and a reduction in hydrolytic and proteolytic activities compared with those of resting macrophages (Yates *et al.*, 2007; Trost *et al.*, 2009). In contrast, some proteins involved in MHC class I and II antigen presentation are enriched in the phagosomes of these cells, resulting in an upregulation of antigen cross-presentation mediated by MHC class I molecules (Trost *et al.*, 2009). In classically activated (M1) human macrophages, the phagosome interior is not acidified but rather maintained near neutral levels (its average pH is ~7.5); this is unlike what happens in alternatively activated (M2) macrophages (Canton *et al.*, 2014). Similarly to M1 macrophages, a neutral phagosomal pH has also been reported in dendritic cells, and this is both required for efficient antigen presentation (Savina *et al.*, 2006, 2009; Jancic *et al.*, 2007; Mantegazza *et al.*, 2008) and achieved by the Rab27A-mediated recruitment of NOX2 components into phagosomes (Jancic *et al.*, 2007). The important implication of our results is that phagosome maturation may be critically regulated by the phosphorylation state of phagosomal SNAP-23 in activated macrophages. Recently, phosphorylation of phagosomal SNAP-23 by IKK2 in dendritic cells was shown to promote the recruitment of the MHC class I molecule, H2-K^b, into phagosomes containing LPS-coated microbeads for efficient cross-presentation (Nair-Gupta *et al.*, 2014). Although there is no sufficient evidence implicating Toll-like receptor signaling in IFN-γ–activated macrophages, the phosphorylation of SNAP-23 at Ser95 by IKK2 may contribute to the development of a favorable phagosomal environment for antigen presentation by delaying fusion with acidic organelles such as lysosomes. In addition, the delay observed in J774 cells overexpressing SNAP-23-S95D may be explained by inhibition of the formation of the acceptor complex consisting of endogenous SNAP-23 and SNARE partner(s) for phagosome maturation (Figure 2C).

Phagosome maturation in macrophages is regulated by several SNARE proteins other than SNAP-23, such as syntaxin 7 (late endosomes), syntaxin 13 (recycling endosomes) (Collins *et al.*, 2002), and VAMP7 (late endosomes/lysosomes) (Sakurai *et al.*, 2012). In dendritic cells, the involvement of Sec22b, which can be found in the endoplasmic reticulum (ER) and the ER-Golgi intermediate complex, in phagosome maturation and antigen cross-presentation is under debate (Cebrian *et al.*, 2011; Wu *et al.*, 2017). Recently, *Escherichia coli* particles and LPS-coated microbeads have been shown to induce IKK2-dependent phosphorylation of phagosomal SNAP-23 (at least at Ser95) in murine dendritic cells, a phosphorylation event that plays a critical role in cross-presentation by mediating the fusion of phagosomes with the endocytic recycling compartment (ERC) containing H2-K^b (Nair-Gupta *et al.*, 2014). In this case, the observed recruitment of two ERC-localized SNAREs, VAMP3 and VAMP8, onto phagosomes containing LPS-coated beads suggests that these SNARE proteins may be binding partners of phosphorylated SNAP-23. Our previous FRET analyses suggested that VAMP7 may be involved in phagosome maturation because its ectopic expression caused a structural alteration of phagosomal SNAP-23 (Sakurai *et al.*, 2012). Since IFN-γ–activated macrophages exhibit enhanced cross-presentation (Trost *et al.*, 2009), phosphorylation of SNAP-23 on phagosomes containing IgG-opsonized particles may result in VAMP7 (which participates in fusion with late endosomes/lysosomes) being replaced by VAMP3 or VAMP8 (which are involved in fusion with ERC) as the preferred SNARE partner of SNAP-23. Phosphorylated SNAP-23 on phagosomes may also interact with syntaxin 11, for which phagosomal localization increases in IFN-γ–activated macrophages (Trost *et al.*, 2009), to form a SNARE complex with VAMP3 or VAMP8. Indeed, phosphorylated SNAP-23 in platelets has been shown to interact with syntaxin 11 and VAMP8 (Karim *et al.*, 2013). Although we observed no significant difference between the non-phosphorylatable and phosphomimicking SNAP-23 mutant in terms of their interaction with these SNARE proteins (Supplemental Figures S2 and S4), it is likely that the identification of specific SNARE partner(s) for phosphorylated SNAP-23 may improve our understanding of several selective membrane fusion events that take place during FcR-mediated phagocytosis under the control of the IFN-γ-signaling pathway.

MATERIALS AND METHODS

Antibodies

Polyclonal antibodies against enhanced green fluorescent protein (EGFP), syntaxin 7, syntaxin 11, VAMP3, VAMP5, VAMP7, and phospho-Ser95-SNAP-23 were prepared as described previously (Yasuda *et al.*, 2011; Sakurai *et al.*, 2012). The remaining antibodies were obtained from commercial sources as follows: anti-syntaxin 13 from Stressgen (Victoria, Canada); anti-syntaxin 3, anti-syntaxin 4, and anti-SNAP-23 from Sigma-Aldrich (St. Louis, MO); anti-VAMP8 from Synaptic Systems (Göttingen, Germany); anti-IKK2 (clone 42D1) from Abnova (Taipei, Taiwan); and anti-CD64 (N-19) from Santa Cruz Biotechnology (Santa Cruz, CA).

Cell culture

J774 cells were obtained from the Riken Cell Bank (Tsukuba, Japan) and cultured in RPMI-1640 medium (Wako Pure Chemical Industries, Osaka, Japan) supplemented with 10% fetal bovine serum (FBS) at 37°C in 5% CO_2. J774 cells stably expressing mVenus-SNAP-23 (mV-S23) proteins were maintained in RPMI supplemented with 10% FBS and 2 μM puromycin to maintain selection.

Expression vectors and establishment of stable transfectants

Human SNAP-23 expression plasmids were constructed by subcloning the PCR-generated cDNA fragments into the pmVenus-C1 vector (Sakurai *et al.*, 2012). *VAMP5* and *IKK2* cDNAs were obtained by reverse transcription PCR using total RNA extracted from J774 cells and then cloned into the pcDNA-Myc-C1 vector. The expression vectors pmVenus-SNAP-23-S95A, pmVenus-SNAP-23-S95D, and pcDNA-Myc-IKK2-KD were created by overlapping PCR (Mercurio *et al.*, 1997) and confirmed by DNA sequencing.

J774 cell lines stably expressing mVenus or mVenus-tagged proteins (mV-S23-WT, mV-S23-S95A, or mV-S23-S95D) were established by infection with recombinant retroviruses generated using cDNAs of mVenus or mV-S23 proteins cloned into the pCX4pur vector, as previously described (Akagi *et al.*, 2003).

Analysis of phagocytosis with opsonized Texas Red–conjugated zymosan particles

The opsonized Texas Red–conjugated zymosan assay was performed as described previously (Hatsuzawa *et al.*, 2009; Sakurai *et al.*, 2012). Briefly, zymosan A particles (cat. no. 263-01491; Wako Pure Chemical Industries) were labeled with sulforhodamine 101 (Texas Red) acid chloride (cat. no. S016; Dojindo Molecular Technologies, Inc., Tokyo, Japan) according to the manufacturer's instructions. J774 cells stably expressing mVenus-tagged proteins were incubated for 1 h in the presence or absence of an approximate 30-fold excess of Texas Red–conjugated zymosan particles opsonized with anti-zymosan antibodies. Subsequently, cells were washed with phosphate-buffered saline (PBS) to remove the free particles and then incubated with 0.025% trypan blue to quench the fluorescence of noninternalized particles. Cellular fluorescence was quantified using a Varioskan Flash microplate reader (Thermo Fisher Scientific, Waltham, MA) at an excitation wavelength of 565 nm and emission wavelength of 615 nm. Arbitrary fluorescence units were calculated by subtracting the fluorescence intensity observed in the absence of the zymosan particles from that observed in their presence. Alternatively, for analysis of association efficiency, cells were incubated for 30 min on ice with the particles and then washed thoroughly with PBS to remove the free particles. The fluorescence of the particles associated with the cells was then measured as described previously in this section.

Phagosome-lysosome fusion assay

The phagosome-lysosome fusion assay was performed as described previously (Sakurai *et al.*, 2012). Briefly, 0.75×10^6 untransfected J774 cells or J774 cells expressing mVenus or mVenus-tagged proteins (mV-S23-WT, mV-S23-S95A, or mV-S23-S95D) were plated onto the center of glass-bottom dishes (35 mm in diameter) and labeled overnight at 37°C with 50 µg/ml RB-dextran (MW 10,000 Da; Invitrogen, Carlsbad, CA). The labeling medium was then removed, and cells were chased for 5 h, washed in ice-cold Hanks' balanced salt solution (HBSS), and incubated first for 30 min on ice in the presence of an approximately 20-fold excess of IgG-opsonized latex beads (3.0 µm in diameter) and then incubated at 30°C for 5 min to initiate phagocytosis. Subsequently, cells were washed three times with ice-cold HBSS and then incubated first for 20 min on ice in the presence of Alexa Fluor 633-conjugated goat anti-rabbit secondary antibodies (Invitrogen) to stain the beads outside the cells and then in HBSS containing cytochalasin B (at a final concentration of 20 µM) for 15 min at 30°C. Images were captured using an LSM780meta laser-scanning microscope under low temperature conditions (~6°C). More than 30 phagosomes were counted for each experiment and categorized as RB-dextran-positive or unlabeled phagosomes based on the presence or absence of detectable RB fluorescence signal.

Immunoprecipitation

Immunoprecipitation was performed as described previously (Hatsuzawa *et al.*, 2009; Sakurai *et al.*, 2012). Briefly, after incubation in the presence or absence of IgG-opsonized zymosan particles, lysates from J774 cells stably expressing mVenus-tagged proteins were incubated with an anti-EGFP antibody for 30 min on ice. Protein A-Sepharose beads (GE Healthcare, Tokyo, Japan) were then added, and the mixture was incubated for 16 h at 4°C under gentle rotation. Subsequently, beads were washed with extraction buffer (20 mM HEPES-KOH, pH 7.2, 100 mM KCl, 2 mM EDTA, 1% Triton X-100, 1 mM phenylmethylsulfonyl fluoride, and 1 mM dithiothreitol) and immune complexes were then eluted with SDS–PAGE sample buffer. After SDS–PAGE, the samples were analyzed by Western blotting using Clean-Blot IP Detection Reagent (Thermo Fisher Scientific), according to the manufacturer's instructions. Immunoreactive proteins were visualized using ImmunoStar Zeta (Wako Pure Chemical Industries) on an ImageQuant LAS-4000 system (GE Healthcare).

FRET probes for SNAP-23

FRET probes for SNAP-23 consisted of TagGFPΔC11 (1–227), which lacked 11 C-terminal residues from the pTagGFP2 vector, and TagRFP-t (1–237), in which Ser162 of the pTagRFP-N vector was replaced with Thr, as described previously (Sakurai *et al.*, 2012). Construction of the tG-S1-tR-S2 probe (TagGFPΔC11 [1–227]-SNAP-23 [1–147]-TagRFP-t [1–237]-SNAP-23 [148–211]) and the negative control tG-S1-S2-tR probe (TagGFPΔC11 [1–227]-SNAP-23 [1–211]-TagRFP-t [1–237]) was described previously (Sakurai *et al.*, 2012). The tG-S1-tR-S2 S95A and S95D probes were created by replacing WT SNAP-23 (1–147) with SNAP-23 (1–147) S95A or S95D, respectively.

FRET analysis

FRET probes of SNAP-23 were expressed in J774 cells together with Myc-tagged VAMP5, IKK2, or IKK2-KD using X-tremeGENE HP DNA Transfection Reagent (Roche Diagnostics K.K., Tokyo, Japan) according to the manufacturer's instructions. Fluorescence spectra of the probes on the plasma and phagosomal membranes of living cells were obtained 20 h after transfection using an LSM510meta (or LSM780meta) laser-scanning microscope with a Plan-Apochromat 63×/1.40 oil DIC M27 objective lens (Carl-Zeiss Microscopy, Oberkochen, Germany) at an excitation wavelength of 458 nm. Before performing measurements, the dynamic range at each wavelength was calibrated using a standard solution according to the manufacturer's instructions. Analysis of the spectrum with a fluorescence intensity of ~3000 (or 250) arbitrary units at 505 (or 502) nm was performed using the LSM510meta (or LSM780meta) microscope. FRET efficiency was represented as the 580/505-nm (or 581/502-nm) emission ratio.

Imaging analyses

J774 cells expressing mV-S23-WT, mV-S23-S95A, or mV-S23-S95D were incubated at 37°C for 30 min in the presence of IgG-opsonized Texas Red–conjugated zymosan particles and then washed with HBSS. Images were captured using an LSM510meta microscope, using a Plan-Apochromat 63×/1.40 oil DIC M27 objective lens (Carl-Zeiss Microscopy).

Statistics

Data are presented as the mean ± SE for the number of experiments indicated in the figure legends. Differences between the groups were analyzed by two-tailed, paired Student's *t* tests or by one-way analysis of variance (ANOVA) with Tukey's post-hoc test using GraphPad Prism software (GraphPad Software, San Diego, CA). Statistical significance was defined as $p < 0.05$.

ACKNOWLEDGMENTS

We are grateful to Masami Takahashi of the Kitasato University School of Medicine for gifting the anti-SNAP-23 antibodies and

Mayumi Takeuchi for providing excellent technical assistance. This work was partly performed at the Tottori Bio Frontier managed by Tottori prefecture and supported in part by funding from a Grant-in-Aid for Young Scientists (B) to C.S. (#25860218) from the Japan Society for the Promotion of Science, as well as by support C.S. received from the Takeda Science Foundation. We thank Editage (www.editage.jp) for their help with English language editing.

REFERENCES

Akagi T, Sasai K, Hanafusa H (2003). Refractory nature of normal human diploid fibroblasts with respect to oncogene-mediated transformation. Proc Natl Acad Sci USA 100, 13567–13572.

Alloatti A, Kotsias F, Pauwels AM, Carpier JM, Jouve M, Timmerman E, Pace L, Vargas P, Maurin M, Gehrmann U, *et al.* (2015). Toll-like receptor 4 engagement on dendritic cells restrains phago-lysosome fusion and promotes cross-presentation of antigens. Immunity 43, 1087–1100.

Becker T, Volchuk A, Rothman JE (2005). Differential use of endoplasmic reticulum membrane for phagocytosis in J774 macrophages. Proc Natl Acad Sci USA 102, 4022–4026.

Canton J (2014). Phagosome maturation in polarized macrophages. J Leukoc Biol 96, 729–738.

Canton J, Khezri R, Glogauer M, Grinstein S (2014). Contrasting phagosome pH regulation and maturation in human M1 and M2 macrophages. Mol Biol Cell 25, 3330–3341.

Cebrian I, Visentin G, Blanchard N, Jouve M, Bobard A, Moita C, Enninga J, Moita LF, Amigorena S, Savina A (2011). Sec22b regulates phagosomal maturation and antigen crosspresentation by dendritic cells. Cell 147, 1355–1368.

Collins RF, Schreiber AD, Grinstein S, Trimble WS (2002). Syntaxins 13 and 7 function at distinct steps during phagocytosis. J Immunol 169, 3250–3256.

Fasshauer D, Sutton RB, Brunger AT, Jahn R (1998). Conserved structural features of the synaptic fusion complex: SNARE proteins reclassified as Q- and R-SNAREs. Proc Natl Acad Sci USA 95, 15781–15786.

Haas A (2007). The phagosome: compartment with a license to kill. Traffic 8, 311–330.

Hatsuzawa K, Hashimoto H, Arai S, Tamura T, Higa-Nishiyama A, Wada I (2009). Sec22b is a negative regulator of phagocytosis in macrophages. Mol Biol Cell 20, 4435–4443.

Hatsuzawa K, Tamura T, Hashimoto H, Yokoya S, Miura M, Nagaya H, Wada I (2006). Involvement of syntaxin 18, an endoplasmic reticulum (ER)-localized SNARE protein, in ER-mediated phagocytosis. Mol Biol Cell 17, 3964–3977.

Hepp R, Puri N, Hohenstein AC, Crawford GL, Whiteheart SW, Roche PA (2005). Phosphorylation of SNAP-23 regulates exocytosis from mast cells. J Biol Chem 280, 6610–6620.

Ho YH, Cai DT, Wang CC, Huang D, Wong SH (2008). Vesicle-associated membrane protein-8/endobrevin negatively regulates phagocytosis of bacteria in dendritic cells. J Immunol 180, 3148–3157.

Hong W, Lev S (2014). Tethering the assembly of SNARE complexes. Trends Cell Biol 24, 35–43.

Jahn R, Scheller RH (2006). SNAREs—engines for membrane fusion. Nat Rev Mol Cell Biol 7, 631–643.

Jancic C, Savina A, Wasmeier C, Tolmachova T, El-Benna J, Dang PM, Pascolo S, Gougerot-Pocidalo MA, Raposo G, Seabra MC, *et al.* (2007). Rab27a regulates phagosomal pH and NADPH oxidase recruitment to dendritic cell phagosomes. Nat Cell Biol 9, 367–378.

Joshi S, Singh AR, Zulcic M, Durden DL (2014). A PKC-SHP1 signaling axis desensitizes Fcγ receptor signaling by reducing the tyrosine phosphorylation of CBL and regulates FcγR mediated phagocytosis. BMC Immunol 15, 18.

Jutras I, Desjardins M (2005). Phagocytosis: at the crossroads of innate and adaptive immunity. Annu Rev Cell Dev Biol 21, 511–527.

Jutras I, Houde M, Currier N, Boulais J, Duclos S, LaBoissière S, Bonneil E, Kearney P, Thibault P, Paramithiotis E, *et al.* (2008). Modulation of the phagosome proteome by interferon-gamma. Mol Cell Proteomics 7, 697–715.

Karim ZA, Zhang J, Banerjee M, Chicka MC, Al Hawas R, Hamilton TR, Roche PA, Whiteheart SW (2013). IkappaB kinase phosphorylation of SNAP-23 controls platelet secretion. Blood 121, 4567–4574.

Larsen EC, DiGennaro JA, Saito N, Mehta S, Loegering DJ, Mazurkiewicz JE, Lennartz MR (2000). Differential requirement for classic and novel PKC isoforms in respiratory burst and phagocytosis in RAW 264.7 cells. J Immunol 165, 2809–2817.

Larsen EC, Ueyama T, Brannock PM, Shirai Y, Saito N, Larsson C, Loegering DJ, Weber PB, Lennartz MR (2002). A role for PKC-ε in FcγR-mediated phagocytosis by RAW 264.7 cells. J Cell Biol 159, 939–944.

Liu F, Morris S, Epps J, Carroll R (2002). Demonstration of an activation regulated NF-kappaB/I-kappaBalpha complex in human platelets. Thromb Res 106, 199–203.

Malaver E, Romaniuk MA, D'Atri LP, Pozner RG, Negrotto S, Benzadon R, Schattner M (2009). NF-kappaB inhibitors impair platelet activation responses. J Thromb Haemost 7, 1333–1343.

Mantegazza AR, Magalhaes JG, Amigorena S, Marks MS (2013). Presentation of phagocytosed antigens by MHC class I and II. Traffic 14, 135–152.

Mantegazza AR, Savina, A, Vermeulen M, Perez L, Geffner J, Hermine O, Rosenzweig SD, Faure F, Amigorena S (2008). NADPH oxidase controls phagosomal pH and antigen cross-presentation in human dendritic cells. Blood 112, 4712–4722.

Mercurio F, Zhu H, Murray BW, Shevchenko A, Bennett BL, Li J, Young DB, Barbosa M, Mann M, Manning A, *et al.* (1997). IKK-1 and IKK-2: cytokine-activated IkappaB kinases essential for NF-kappaB activation. Science 278, 860–866.

Murray RZ, Kay JG, Sangermani DG, Stow JL (2005). A role for the phagosome in cytokine secretion. Science 310, 1492–1495.

Nair-Gupta P, Baccarini A, Tung N, Seyffer F, Florey O, Huang Y, Banerjee M, Overholtzer M, Roche PA, Tampé R, *et al.* (2014). TLR signals induce phagosomal MHC-I delivery from the endosomal recycling compartment to allow cross-presentation. Cell 158, 506–521.

Ng Yan Hing JD, Desjardins M, Descoteaux A (2004). Proteiomic analysis reveals a role for protein kinase C-α in phagosome maturation. Biochem Biophys Res Commun 319, 810–816.

Polgar J, Lane WS, Chung SH, Houng AK, Reed GL (2003). Phosphorylation of SNAP-23 in activated human platelets. J Biol Chem 278, 44369–44376.

Puri N, Roche PA (2006). Ternary SNARE complexes are enriched in lipid rafts during mast cell exocytosis. Traffic 7, 1482–1494.

Sakurai C, Hashimoto H, Nakanishi H, Arai S, Wada Y, Sun-Wada GH, Wada I, Hatsuzawa K (2012). SNAP-23 regulates phagosome formation and maturation in macrophages. Mol Biol Cell 23, 4849–4863.

Savina A, Jancic C, Hugues S, Guermonprez P, Vargas P, Moura IC, Lennon-Dumenil AM, Seabra MC, Raposo G, Amigorena S (2006). NOX2 controls phagosomal pH to regulate antigen processing during crosspresentation by dendritic cells. Cell 126, 205–218.

Savina A, Peres A, Cebrian I, Carmo N, Moita C, Hacohen N, Moita LF, Amigorena S (2009). The small GTPase Rac2 controls phagosomal alkalinization and antigen crosspresentation selectively in CD8(+) dendritic cells. Immunity 30, 544–555.

Shcherbo D, Souslova EA, Goedhart J, Chepurnykh TV, Gaintzeva A, Shemiakina II, Gadella TW, Lukyanov S, Chudakov DM (2009). Practical and reliable FRET/FLIM pair of fluorescent proteins. BMC Biotechnol 9, 24.

Stow JL, Manderson AP, Murray RZ (2006). SNAREing immunity: the role of SNAREs in the immune system. Nat Rev Immunol 6, 919–929.

Suzuki K, Verma IM (2008). Phosphorylation of SNAP-23 by IkappaB kinase 2 regulates mast cell degranulation. Cell 134, 485–495.

Trost M, English L, Lemieux S, Courcelles M, Desjardins M, Thibault P (2009). The phagosomal proteome in interferon-gamma-activated macrophages. Immunity 30, 143–154.

Wesolowski J, Paumet F (2014). Escherichia coli exposure inhibits exocytic SNARE-mediated membrane fusion in mast cells. Traffic 15, 516–530.

Wood TR, Chow RY, Hanes CM, Zhang X, Kashiwagi K, Shirai Y, Trebak M, Loegering DJ, Saito N, Lennartz MR (2013). PKC-pseudosubstrate and catalytic activity during IgG-mediated phagocytosis. J Leukoc Biol 94, 109–122.

Wu SJ, Niknafs YS, Kim SH, Oravecz-Wilson K, Zajac C, Toubai T, Sun Y, Prasad J, Peltier D, Fujiwara H, *et al.* (2017). A critical analysis of the role of SNARE proteins SEC22B in antigen cross-presentation. Cell Rep 19, 2645–2656.

Yasuda K, Itakura M, Aoyagi K, Sugaya T, Nagata E, Ihara H, Takahashi M (2011). PKC-dependent inhibition of CA2+-dependent exocytosis from astrocytes. Glia 59, 143–151.

Yates RM, Hermetter A, Taylor GA, Russell DG (2007). Macrophage activation downregulates the degradative capacity of the phagosome. Traffic 8, 241–250.